Evidence that Phospholipids Play a Key Role in Pre-β ApoA-I Formation and High-Density Lipoprotein Remodeling†

Kerry-Anne Rye,*,‡ MyNgan Duong,‡,§ Maria K. Psaltis,‡ Linda K. Curtiss,|| David J. Bonnet,|| Roland Stocker,⊥ and Philip J. Barter‡,§

Lipid Research Laboratory, Hanson Institute, Adelaide, South Australia, Australia 5000, University of Adelaide, Department of Medicine, Royal Adelaide Hospital, South Australia, Australia 5000, Department of Immunology, The Scripps Research Institute, La Jolla, California 92037, and Centre for Thrombosis and Vascular Research, School of Medical Sciences, University of New South Wales, Sydney, New South Wales, Australia 2050

Received April 22, 2002; Revised Manuscript Received August 15, 2002

ABSTRACT: The initial plasma acceptor of unesterified cholesterol and phospholipids from peripheral cells has been identified as pre-β migrating, lipid-free, or lipid-poor apolipoprotein (apo) A-I (pre-β apoA-I). Pre-β apoA-I is formed when plasma factors, such as cholesteryl ester transfer protein (CETP), remodel high-density lipoproteins (HDL). The aim of this study is to determine how phospholipids influence pre-β apoA-I formation during the CETP-mediated remodeling of HDL. Reconstituted HDL (rHDL) containing either 1-palmitoyl-2-oleoyl phosphatidylcholine (POPC), 1-palmitoyl-2-linoleoyl phosphatidylcholine (PLPC), 1-palmitoyl-2-arachidonyl phosphatidylcholine (PAPC), or 1-palmitoyl-2-docosahexanoyl phosphatidylcholine (PDPC) as the only phospholipid were prepared. The rHDL were comparable in size and core lipid/protein molar ratio and contained only cholesteryl esters in their core and apoA-I as the sole apolipoprotein. The (POPC)rHDL, (PLPC)rHDL, (PAPC)rHDL, and (PDPC)rHDL were respectively incubated for 0−24 h with CETP and microemulsions containing triolein and either POPC, PLPC, PAPC, or PDPC. The rate at which the rHDL were depleted of core lipids and remodeled to small particles varied widely with (POPC)rHDL < (PLPC)rHDL < (PDPC)rHDL ∼ (PAPC)rHDL. Pre-β apoA-I was not formed in the (POPC)rHDL incubations. Pre-β apoA-I was apparent by 24 h in the (PLPC)rHDL incubations and by 12 h in the (PAPC)rHDL and (PDPC)rHDL incubations. The enhanced formation of pre-β apoA-I in the (PAPC)rHDL and (PDPC)rHDL incubations reflected the increased core lipid depletion of the particles combined with the destabilization and progressive exclusion of apoA-I from the particle surface. In conclusion, these results show that phospholipids play a key role in the CETP-mediated remodeling of rHDL and pre-β apoA-I formation.

Several mechanisms contribute to the cardioprotective properties of high-density lipoproteins (HDL)[1]. These include the antioxidant properties of HDL (*1*), the ability of HDL to inhibit cytokine-induced endothelial cell adhesion molecule expression (*2*), and the role of HDL in the potentially antiatherogenic pathway of reverse cholesterol transport (*3*).

Reverse cholesterol transport involves the removal of cholesterol from cells and its transport to the liver for excretion. The first step in this pathway is the efflux of unesterified cholesterol (UC) and phospholipids from peripheral cells to pre-β migrating lipid-poor or lipid-free apolipoprotein (apo) A-I (pre-β apoA-I) (*4*). This process depends on the presence of the ATP-binding cassette transporter protein, ABCA1, in the cell membrane (*5*). While the mechanism of the ABCA1-mediated efflux of UC and phospholipids to pre-β apoA-I is the subject of intense investigation, the origins of pre-β apoA-I, and how their formation is regulated, is poorly understood.

Pre-β apoA-I are formed when HDL are remodeled by plasma factors such as cholesteryl ester transfer protein (CETP) and phospholipid transfer protein (*6*, *7*). The aims of the present study were to determine if phospholipids play a role in pre-β apoA-I formation during the CETP-mediated remodeling of HDL. To achieve these aims, it was important to use HDL that varied systematically in phospholipid composition. HDL from human plasma could not be used because of the intrinsic heterogeneity of their phospholipids. Although phosphatidylcholine (PC) is the most abundant phospholipid in plasma HDL, it also contains significant amounts of other phospholipid classes (*8*). HDL PC acyl chains also vary in length and unsaturation, with 1-palmitoyl-2-oleoyl phosphatidylcholine (POPC), 1-palmitoyl-2-linoleoyl phosphatidylcholine (PLPC), 1-palmitoyl-2-arachidonyl

† This work was supported by the National Health and Medical Research Council of Australia Grant 9936240 and NIH Grant HL43815.

* Corresponding author. Tel: +61-8-8222-3448. Fax: +61-8-8222-3154. E-mail: karye@ozemail.com.au.

‡ Hanson Institute.

§ University of Adelaide.

|| The Scripps Research Institute.

⊥ University of New South Wales.

[1] Abbreviations: apoA-I, apolipoprotein A-I; CE, cholesteryl esters; CETP, cholesteryl ester transfer protein; CO, cholesteryl oleate; HDL, high-density lipoprotein(s); LCAT, lecithin:cholesterol acyltransferase; PC, phosphatidylcholine; PAPC, 1-palmitoyl-2-arachidonyl phosphatidylcholine; PDPC, 1-palmitoyl-2-docosahexanoyl phosphatidylcholine; PLPC, 1-palmitoyl-2-linoleoyl phosphatidylcholine; POPC, 1-palmitoyl-2-oleoyl phosphatidylcholine; rHDL, reconstituted HDL; TBS, Tris-buffered saline; TO, triolein; UC, unesterified cholesterol.

10.1021/bi025998k CCC: $22.00
Published on Web 09/18/2002

phosphatidylcholine (PAPC), and 1-palmitoyl-2-docosahexanoyl phosphatidylcholine (PDPC) comprising 12.9%, 34.4%, 9.1%, and 3.6%, respectively, of the total HDL PC (*9*). One consequence of this heterogeneity is that, irrespective of whether HDL are isolated from human plasma on the basis of size, charge, or apolipoprotein composition, particles containing mixtures of phospholipids are always obtained.

To overcome this problem, a new approach for preparing spherical reconstituted HDL (rHDL) with a single type of PC was developed specifically for this study. The rHDL contained apoA-I as the only apolipoprotein, cholesteryl esters (CE) as the only core lipid, and either POPC, PLPC, PAPC, or PDPC as the only phospholipid. When these preparations were respectively incubated with CETP and microemulsions containing triolein (TO) and either POPC, PLPC, PAPC, or PDPC, it was evident that phospholipids play a key role in the CETP-mediated remodeling of rHDL and pre-β apoA-I formation.

EXPERIMENTAL PROCEDURES

Preparation of ApoA-I, Lecithin:Cholesterol Acyltransferase (LCAT) and CETP. ApoA-I was purified from human plasma as described (*10, 11*). Preparations of LCAT with activities ranging from 1 to 2.4 μmol CE/mL LCAT/h were isolated as described and concentrated 10-fold by ultrafiltration (Amicon, Danvers, MA) (*12*). CETP preparations with activities ranging from 21.2 to 39.0 units/mL were prepared as described (*13*).

Preparation of Spherical rHDL. Discoidal rHDL containing UC, apoA-I, and either POPC, PLPC, PAPC, or PDPC (initial PC/UC/apoA-I molar ratio 110:5:1) were prepared by cholate dialysis (*14*) and dialyzed against Tris-buffered saline (TBS) (10 mM Tris, 150 mM NaCl), pH 7.4, containing 50 μM diethylenetriamine pentaacetic acid, 0.006% (w/v) and 10 μM butylated hydroxytoluene. Chelex 100 resin (Bio-Rad, Hercules, CA) (2 g/L) was added to the TBS to prevent inadvertent oxidation.

Discoidal rHDL were converted into spherical rHDL by incubation with LCAT, and UC in ethanol. In a typical incubation, discoidal (POPC)rHDL (final UC concentration 0.2 mM/L), BSA (final concentration 40 mg/mL), β-mercaptoethanol (final concentration 4 mM/L), and LCAT (2.6 mL of a preparation that esterified 1.1 μmol CE/mL LCAT/h) were incubated at 37 °C for 30 min. The volume of the incubation mixture was 10.1 mL.

At 30 min, 0.052 mL of 24.6 mM/L UC in ethanol and an additional 0.65 mL of LCAT were added to the incubation mixture. Extra BSA and β-mercaptoethanol were also added so that their respective concentrations were maintained at 40 mg/mL and 4 mM/L. The additions of UC, LCAT, BSA, and β-mercaptoethanol were repeated at 30 min intervals until 7 h had elapsed. The incubation was continued without further additions for a total of 24 h. The final volume of the incubation mixture was 23.4 mL. The spherical (POPC)rHDL were isolated by ultracentrifugation ($1.07 < d < 1.21$ g/mL) and dialyzed against TBS. Activity of LCAT was not detected in the isolated rHDL.

The amount of LCAT required to prepare spherical rHDL varied according to the discoidal rHDL PC composition. This reflects variations in the substrate specificity of LCAT (*15*). While a total of 11.8 mL of LCAT was needed to convert discoidal (POPC)rHDL into spherical (POPC)rHDL, the conversion of an equivalent amount of discoidal (PLPC)-rHDL into spherical (PLPC)rHDL required 10.0 mL of the same preparation of LCAT. For the (PAPC)rHDL, 21.7 mL of the same LCAT was needed to convert disks into spheres, while 42.2 mL of LCAT was required to prepare spherical (PDPC)rHDL.

Preparation of Microemulsions. Microemulsions containing triolein (TO) and either POPC, PLPC, PAPC, or PDPC were prepared by sonication (*16*). The same approach was also used to prepare microemulsions with cholesteryl oleate (CO) and either POPC, PLPC, PAPC, or PDPC.

Preparation of CO-Enriched Spherical rHDL. Spherical (PLPC)rHDL, (PAPC)rHDL, and (PDPC)rHDL (final CE concentration 0.1 mM/L) were incubated at 37 °C for 1 h with CETP (2.7 units/mL) and microemulsions, respectively, containing CO and either PLPC, PAPC, or PDPC (final CO concentration 4.0 mM/L). Control incubations were carried out in the absence of CETP. When the incubations were complete, the rHDL were isolated by ultracentrifugation ($1.07 < d < 1.21$ g/mL) and dialyzed against TBS.

Determination of rHDL CE Composition. Spherical rHDL CE composition was determined by HPLC with UV_{210nm} detection (*17*). In brief, the rHDL were extracted with methanol/hexane, and the organic phase was separated, dried, and then resuspended in methanol/tert.butyl alcohol (1/1, v/v). Lipids were separated by reverse-phase HPLC and individual CE quantified at 210 nm by area comparison with authentic standards (Sigma).

Spectroscopic Studies. Intrinsic fluorescence emission spectra of the rHDL were obtained as described (*13*). The concentration of GdnHCl required to unfold apoA-I by 50% was determined by incubating the rHDL at 25 °C for 24 h with 0−8.0 M GdnHCl and plotting the wavelength of maximum fluorescence versus the concentration of GdnHCl (*12*). The kinetics of unfolding of apoA-I was determined by measuring the wavelength of maximum fluorescence of rHDL incubated at 25 °C for 0−24 h with 3.5 M GdnHCl. PC acyl chain packing order was determined as the steady-state fluorescence polarization of 1,6-diphenyl-1,3,5-hexatriene-labeled rHDL at 5 °C intervals from 5 to 45 °C (*12*). All spectroscopic data represent the mean ± sd of triplicate determinations.

Mass spectra were acquired with an API-100 ion spray mass spectrometer (PE/Sciex) using an ion source voltage equal to 5000 V and an orifice voltage of 70 V. Data were collected at 0.1 amu resolution over a mass/charge (m/z) range of 100−1000.

Surface Plasmon Resonance Analysis. A Biacore 2000 biosensor (Pharmacia) was used to measure the association rate constant (ka) of each rHDL for six unique apoA-I-specific monoclonal antibodies. Maximum amounts of rabbit antimouse Fc (RAM-Fc) were immobilized on all four flowcells of a CM5 chip using amine coupling (*18*). Each rHDL (analyte) was then bound by the captured antibodies. Following covalent attachment of the RAMFc, purified antibodies were injected individually at 1.9−10 μg/mL protein to give approximately 400 response units.

Data were collected at a high rate (10 Hz). Data evaluation began by synchronizing the injection times and zeroing each sensorgram to baseline. For each antibody and rHDL combination, a set of sensorgrams was evaluated with a 1:1

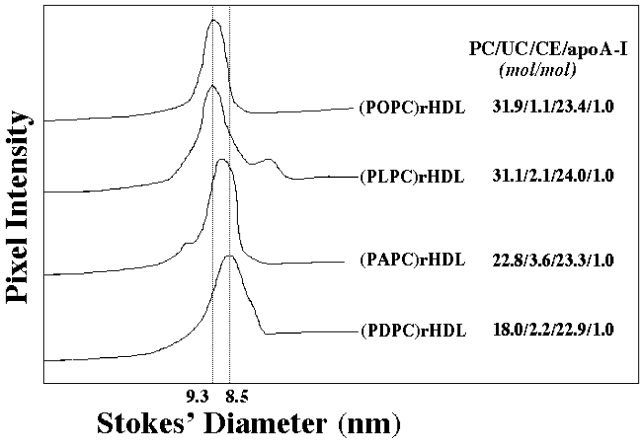

FIGURE 1: Physical properties of spherical (POPC)rHDL, (PLPC)-rHDL, (PAPC)rHDL, and (PDPC)rHDL. The rHDL were subjected to nondenaturing polyacrylamide gradient gel electrophoresis. Scans of Coomassie-stained gels are shown. Diameters were determined by reference to high molecular weight standards of known diameter. Stoichiometries were calculated from the concentrations of individual constituents.

(Langmuir) association (*k* observed) model. The k_a was obtained from the slope of the plot of *k* observed versus analyte concentration.

Other Techniques. Spherical rHDL surface charge and size were respectively determined by agarose gel electrophoresis and nondenaturing 3/40% polyacrylamide gradient gel electrophoresis (*13*). 2-D gel electrophoresis (agarose gel electrophoresis followed by nondenaturing polyacrylamide gradient gel electrophoresis) was carried out as described (*19*). For immunoblotting the rHDL were electrophoretically transferred to nitrocellulose membranes, and apoA-I was detected by enhanced chemiluminescence (Amersham Life Sciences, Inc) (*6*).

A Cobas Fara automated analyzer (Roche Diagnostics, Switzerland) was used for all chemical analyses. ApoA-I concentrations were determined as described using BSA as a standard (*20*). Enzymatic kits (Boehringer Mannheim, GmbH, Germany) were used to measure PC, UC, and total cholesterol concentrations. All concentrations were determined in triplicate. The number of apoA-I molecules/rHDL was determined by cross linking (*21*).

Statistical Analysis. The data analysis package in Microsoft Excel 2000 was used for statistical analyses. The *t*-test for two-tailed distribution and two-sample unequal variance (heteroscedastic) was used to determine significant differences. ANOVA: Two-factor with repeated measures was used to assess differences between data sets. Significance was set at $p < 0.05$.

RESULTS

Physical Properties of Spherical rHDL (Figure 1). As judged by nondenaturing gradient gel electrophoresis, the (POPC)rHDL and (PLPC)rHDL were 9.3 nm in diameter (Figure 1). The respective diameters of the (PAPC)rHDL and (PDPC)rHDL were 9.0 and 8.5 nm. CE/apoA-I molar ratios ranged from 22.9/1.0 for (PDPC)rHDL to 24.0/1.0 for (PLPC)rHDL. PC/apoA-I molar ratios varied from 18.0/1.0 for (PDPC)rHDL to 31.9/1.0 for (POPC)rHDL. As judged by covalent cross linking, all of the rHDL contained three apoA-I molecules/particle (not shown). Lysophosphatidylcholine was not detected in any of the rHDL by mass spectroscopy (not shown).

The rHDL CE composition was determined by HPLC. The (POPC)rHDL contained only CO. The (PLPC)rHDL contained 14.4% cholesteryl palmitate and 85.6% cholesteryl linoleate. The (PAPC)rHDL contained 8.2% cholesteryl palmitate and 91.8% cholesteryl arachidonate. The (PDPC)-rHDL contained 7.6% cholesteryl palmitate and 92.4% cholesteryl docosahexanoate.

Remodeling of rHDL by CETP (Table 1, Figures 2 and 3). The rHDL were incubated for 0−24 h with CETP and PC/TO microemulsions. To ensure that their PC composition did not change, the (POPC)rHDL, (PLPC)rHDL, (PAPC)-rHDL, and (PDPC)rHDL were respectively incubated with microemulsions containing either POPC, PLPC, PAPC, or PDPC.

When the rHDL were incubated with the microemulsions alone, their PC/apoA-I molar ratios increased as a consequence of spontaneous transfers of PC from the microemulsions to the rHDL (Table 1). When CETP was present in the incubations, there was a time-dependent decrease in the rHDL CE/apoA-I molar ratios (Table 1 and Figure 2, closed circles) and a concomitant increase in the TO/apoA-I molar ratios (Table 1 and Figure 2, open circles). At 24 h, CE was the predominant (POPC)rHDL core lipid. The (PLPC)rHDL was depleted of CE at 24 h, while the (PAPC)rHDL and (PDPC)rHDL were depleted of CE at 12 h.

The rHDL (CE + TO)/apoA-I molar ratios were calculated from the data in Table 1, normalized to 100% at $T = 0$ h and plotted as a function of time (Figure 2, insets). At 24 h the (POPC)rHDL and (PLPC)rHDL core lipids had decreased by 15% and 62%, respectively, compared to a 79% reduction for the (PAPC)rHDL and (PDPC)rHDL. As similar amounts of triolein were transferred from the microemulsions to the rHDL, the variations in core lipid depletion reflect different amounts of cholesteryl esters transferred from rHDL to the microemulsions. The mechanism underlying the CETP-mediated reduction in rHDL core lipid content has been addressed in previous work from this laboratory (*13*).

Changes in rHDL size were assessed by nondenaturing gradient gel electrophoresis (Figure 3a). Profiles A and B respectively show rHDL's that were either maintained at 4 °C or incubated at 37 °C for 24 h with microemulsions alone. Profiles C−G respectively show the rHDL after incubation with microemulsions and CETP for 1, 3, 6, 12, and 24 h. Incubation with the microemulsions alone did not affect (POPC)rHDL or (PLPC)rHDL size. When CETP was included in the incubations, approximately 38% of the (POPC)rHDL and 70% of the (PLPC)rHDL were remodeled to small particles by 24 h.

The (PAPC)rHDL and (PDPC)rHDL increased in size when they were incubated with the microemulsions alone. This reflects the spontaneous transfer of phospholipids from the PAPC/TO and PDPC/TO microemulsions to the rHDL. When CETP was present in the incubations, approximately 65% of the (PAPC)rHDL and 78% of the (PDPC)rHDL were remodeled to small particles by 24 h.

To determine if the loss of core lipids and reduction in particle size caused apoA-I to dissociate from the rHDL, the incubation mixtures were subjected to nondenaturing gradient gel electrophoresis and immunoblotted for apoA-I (Figure 3b). The rHDL that were either maintained at 4 °C or

Table 1: Stoichiometry of rHDL after Incubation with CETP and PC/TO Microemulsions[a]

rHDL	additions	incubation conditions	stoichiometry (mol/mol) PC	UC	CE	TG	apoA-I
POPC	(POPC) microemulsion, −CETP	4 °C, 24 h	31.9 ± 0.9	1.1 ± 0.1	23.4 ± 0.5	0.0	1.0
	(POPC) microemulsion, −CETP	37 °C, 24 h	39.1 ± 1.0	1.7 ± 0.4	26.6 ± 0.9	0.0	1.0
	(POPC) microemulsion, +CETP	37 °C, 1 h	39.7 ± 0.5	1.8 ± 0.4	26.1 ± 0.9	1.3 ± 0.3	1.0
	(POPC) microemulsion, +CETP	37 °C, 3 h	40.1 ± 1.3	1.5 ± 0.1	23.7 ± 0.3	2.9 ± 0.1	1.0
	(POPC) microemulsion, +CETP	37 °C, 6 h	41.6 ± 0.7	1.6 ± 0.1	19.4 ± 0.4	5.3 ± 0.5	1.0
	(POPC) microemulsion, +CETP	37 °C, 12 h	43.8 ± 0.4	1.8 ± 0.1	17.7 ± 0.5	8.3 ± 0.4	1.0
	(POPC) microemulsion, +CETP	37 °C, 24 h	48.9 ± 1.6	1.8 ± 0.4	13.8 ± 0.0	8.8 ± 0.4	1.0
PLPC	(PLPC) microemulsion, −CETP	4 °C, 24 h	31.1 ± 0.5	2.1 ± 0.1	21.0 ± 2.1	0.0	1.0
	(PLPC) microemulsion, −CETP	37 °C, 24 h	34.2 ± 1.1	2.5 ± 0.2	20.3 ± 1.1	0.0	1.0
	(PLPC) microemulsion, +CETP	37 °C, 1 h	31.3 ± 0.8	2.8 ± 0.1	13.8 ± 1.8	1.0 ± 0.2	1.0
	(PLPC) microemulsion, +CETP	37 °C, 3 h	31.2 ± 0.8	2.6 ± 0.1	13.4 ± 1.2	1.1 ± 0.2	1.0
	(PLPC) microemulsion, +CETP	37 °C, 6 h	32.4 ± 0.3	0.0	12.3 ± 0.3	2.9 ± 0.6	1.0
	(PLPC) microemulsion, +CETP	37 °C, 12 h	35.7 ± 1.0	3.6 ± 0.1	4.1 ± 1.2	5.0 ± 0.3	1.0
	(PLPC) microemulsion, +CETP	37 °C, 24 h	35.5 ± 0.3	2.8 ± 0.1	1.2 ± 0.5	6.2 ± 0.4	1.0
PAPC	(PAPC) microemulsion, −CETP	4 °C, 24 h	22.8 ± 0.4	3.6 ± 0.2	24.5 ± 1.7	0.0	1.0
	(PAPC) microemulsion, −CETP	37 °C, 24 h	34.7 ± 0.6	3.3 ± 0.2	23.3 ± 1.5	0.0	1.0
	(PAPC) microemulsion, +CETP	37 °C, 1 h	31.7 ± 1.1	3.6 ± 0.4	5.9 ± 2.0	7.0 ± 0.3	1.0
	(PAPC) microemulsion, +CETP	37 °C, 3 h	35.3 ± 0.2	6.3 ± 0.2	5.5 ± 1.3	5.6 ± 0.4	1.0
	(PAPC) microemulsion, +CETP	37 °C, 6 h	38.0 ± 1.7	3.8 ± 0.1	3.3 ± 0.9	7.6 ± 0.5	1.0
	(PAPC) microemulsion, +CETP	37 °C, 12 h	41.1 ± 0.6	4.2 ± 0.4	0.7 ± 0.4	7.8 ± 0.4	1.0
	(PAPC) microemulsion, +CETP	37 °C, 24 h	41.9 ± 0.9	0.0	0.6 ± 0.3	4.9 ± 0.8	1.0
PDPC	(PDPC) microemulsion, −CETP	4 °C, 24 h	18.0 ± 0.3	2.2 ± 0.1	22.9 ± 0.0	0.0	1.0
	(PDPC) microemulsion, −CETP	37 °C, 24 h	32.3 ± 0.5	2.7 ± 0.1	20.8 ± 0.8	0.0	1.0
	(PDPC) microemulsion, +CETP	37 °C, 1 h	31.5 ± 1.3	2.5 ± 0.1	6.6 ± 1.1	4.5 ± 0.3	1.0
	(PDPC) microemulsion, +CETP	37 °C, 3 h	35.4 ± 0.8	3.0 ± 0.0	1.8 ± 0.6	6.1 ± 0.2	1.0
	(PDPC) microemulsion, +CETP	37 °C, 6 h	35.1 ± 1.0	2.9 ± 0.1	1.4 ± 0.4	6.3 ± 0.2	1.0
	(PDPC) microemulsion, +CETP	37 °C, 12 h	35.1 ± 1.7	4.0 ± 0.2	0.0	4.5 ± 0.4	1.0
	(PDPC) microemulsion, +CETP	37 °C, 24 h	33.5 ± 0.2	4.0 ± 0.2	0.2 ± 0.1	3.3 ± 0.5	1.0

[a] The rHDL were mixed with PC/TO microemulsions and incubated in the presence or absence of CETP as described in the legend to Figure 2. The composition (mean ± s.d., $n = 3$) of the rHDL at each time point is shown.

incubated at 37 °C for 24 h with the microemulsions alone are respectively shown in Tracks A and B. Tracks C−G show rHDL that were incubated with microemulsions and CETP for 1, 3, 6, 12, and 24 h. Lipid-free apoA-I is shown in Track H. ApoA-I did not dissociate from the (POPC)rHDL. ApoA-I dissociated from the (PLPC)rHDL by 24 h and from the (PAPC)rHDL and (PDPC)rHDL by 12 h.

The mass of pre-β apoA-I formed when the (PLPC)rHDL, (PAPC)rHDL, and (PDPC)rHDL were incubated for 24 h with CETP and their respective microemulsions was estimated by scanning the immunoblots in Figure 3b and calculating the areas under the curves. Pre-β apoA-I accounted for 24%, 38%, and 35% of the total apoA-I in the (PLPC)rHDL, (PAPC)rHDL, and (PDPC)rHDL incubations, respectively.

To determine if the dissociated apoA-I was comparable in size and charge to pre-β apoA-I, the rHDL that had been incubated with microemulsions and CETP for 24 h were subjected to 2-D gel electrophoresis (Figure 3c, Panel A). A sample of lipid-free apoA-I was also applied to the gradient gels (Figure 3c, Panel B). The apoA-I that dissociated from the (PLPC)rHDL, (PAPC)rHDL and (PDPC)rHDL (arrows) comigrated with lipid-free apoA-I on the gradient gel. This confirms its identity as pre-β apoA-I. Pre-β apoA-I was not detected in the (POPC)rHDL sample.

As noted above, the rHDL CE acyl esters varied in length and unsaturation. To make sure that these differences did not impact on the particle remodeling or pre-β apoA-I formation, the (PLPC)rHDL, (PAPC)rHDL, and (PDPC)-rHDL were enriched with CO. Enrichment with CO had no effect on rHDL size and was not associated with a nett loss of core lipids (not shown). As judged by HPLC, the CO-enriched (PLPC)rHDL contained 87.5% CO and 12.5% cholesteryl linoleate. The CO-enriched (PAPC)rHDL contained 89.3% CO and 10.7% cholesteryl arachidonate, while the CO-enriched (PDPC)rHDL contained 89.4% CO and 10.6% cholesteryl docosahexanoate.

When the CO-enriched rHDL were incubated with CETP and PC/TO microemulsions, core lipid transfers, changes in particle size and the dissociation of apoA-I were indistinguishable from what is shown in Figures 2 and 3 for the unmodified rHDL.

Mechanism of Pre-β ApoA-I Formation (Figures 4 and 5). As judged by agarose gel electrophoresis, the surface charge of the (POPC)rHDL and (PLPC)rHDL was comparable to that of plasma HDL ($-0.54\ \mu m\ s^{-1}\ V^{-1}$ cm). The respective surface charges of (PAPC)rHDL and (PDPC)-rHDL were -0.67 and $-0.64\ \mu m\ s^{-1}\ V^{-1}$ cm. This suggested that the conformation of apoA-I was not the same in all the rHDL preparations.

This possibility was investigated further by determining the intrinsic wavelengths of maximum fluorescence of the samples. The respective values for the (POPC)rHDL, (PLPC)-rHDL, and (PAPC)rHDL were 333.7 ± 0.8, 334.3 ± 0.3, and 335.5 ± 0.5 nm. The value for (PDPC)rHDL, 336.3 ± 0.8 nm, was comparable to that of lipid-free apoA-I (336.1 ± 1.0 nm). This indicated that the apoA-I Trp residues become more exposed to the aqueous environment with increasing rHDL PC acyl chain length and unsaturation. Increased exposure of apoA-I Trp residues with increasing length and unsaturation of PC acyl chains has also been reported for discoidal rHDL (*22*).

This could be explained by the more unsaturated PC acyl chains becoming increasingly disordered and progressively

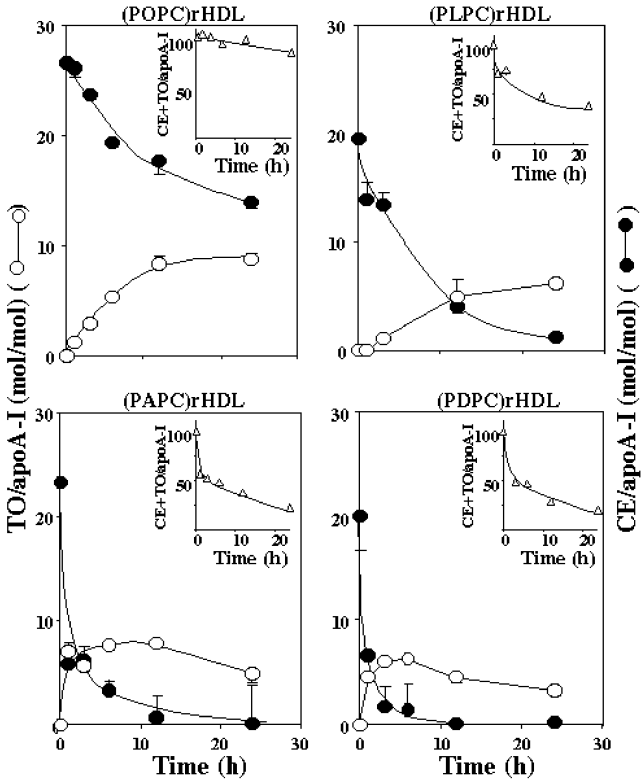

FIGURE 2: Remodeling of rHDL by CETP: Core lipid transfers. PC/TO microemulsions and rHDL were incubated in the presence or absence of CETP. The final concentrations of rHDL CE and microemulsion TO were 0.1 and 4.0 mM/L, respectively. The samples without CETP were either maintained at 4 °C or incubated at 37 °C for 24 h. Samples containing CETP (final activity 2.7 units/mL) were incubated at 37 °C for 1, 3, 6, 12, or 24 h. The final volume was 2 mL. After incubation the rHDL were isolated by ultracentrifugation ($1.07 < d < 1.21$ g/mL). CE/apoA-I (●) and TO/apoA-I (○) molar ratios are shown. Insets show the (CE + TO)/apoA-I molar ratio at each time point.

excluding the apoA-I from the rHDL surface. This, in turn, could reduce the stability of the apoA-I and facilitate its dissociation from the rHDL. The first of these possibilities was investigated by labeling the rHDL with 1,6-diphenyl-1,3,5-hexatriene and monitoring PC acyl chain packing order by steady-state fluorescence polarization. These results established that the polarization of (POPC)rHDL > (PLPC)-rHDL > (PAPC)rHDL > (PDPC)rHDL (not shown). The same hierarchy has been reported for discoidal rHDL (*22*). As judged by ANOVA, the differences between the spherical (PAPC)rHDL and the spherical (PDPC)rHDL were significant at the level of $p < 0.01$. The other differences were significant at the level of $p < 0.001$. This confirms that the packing order of spherical rHDL PC acyl chains decreases as their unsaturation increases.

To determine if the stability of apoA-I also decreased, the rHDL were incubated for 0−24 h with 3.5 M GdnHCl (Figure 4). The rate of unfolding of apoA-I varied widely, with (PDPC)rHDL (closed diamonds) > (PAPC)rHDL (closed circles) > (PLPC)rHDL (closed triangles) > (POPC)-rHDL (closed squares). The unfolding of a control sample of lipid-free apoA-I is also shown (open circles). The concentration of GdnHCl required to unfold apoA-I by 50% was also determined. Lipid-free apoA-I was unfolded by 50% in the presence of 0.9 ± 0.1 M GdnHCl, compared to 1.5 ± 0.1 M for the apoA-I in (PDPC)rHDL, 2.0 ± 0.1 M GdnHCl for (PLPC)rHDL, and (PAPC)rHDL and 3.8 ± 0.1 M GdnHCl for (POPC)rHDL. This indicated that the stability of apoA-I decreased as the spherical rHDL PC *sn*-2 acyl chains became increasingly disordered. This is consistent with what been reported for the apoA-I in discoidal (POPC)-rHDL, (PLPC)rHDL, (PAPC)rHDL, and (PDPC)rHDL (*22*).

Surface plasmon resonance was used to identify the regions of apoA-I in which the conformation varied (Figure 5). Six unique epitopes between the N- and the C- terminal regions of apoA-I were examined. The immediate N-terminal epitope of apoA-I (aa residues 1−19) had a higher affinity for its antibody on (PDPC)rHDL compared with the other rHDL. By contrast, compared with all other rHDL, the three C-terminal epitopes of (PDPC)rHDL, defined by aa residues 178−200, aa residues 187−210, and the immediate C-terminal epitope comprising residues 220−242, had significantly lower affinities for their respective antibodies. This suggested that the N-terminal region of apoA-I in (PDPC)-rHDL is more exposed than the C-terminal region of apoA-I in (POPC)rHDL and is consistent with the fluorescence spectroscopic data. Interestingly, the affinity of two adjoining regions of apoA-I (epitopes 96−111 and 115−126) changed in opposite directions. The largest differences between (POPC)rHDL, (PLPC)rHDL, and (PAPC)rHDL were at epitope 115−126, which represents a proline-punctuated β-turn between adjoining α-helices. These results indicate that rHDL PC acyl chain composition affects the conformation of multiple domains along the entire length of the apoA-I molecule.

DISCUSSION

Reverse cholesterol transport is a potentially anti-atherogenic process whereby UC and phospholipids are removed from cells and transported by HDL to the liver for excretion (*3*). The initial step in this process is the efflux of UC and phospholipids from cell membranes that express the ATP-binding cassette transporter, ABCA1, to pre-β migrating, lipid-poor, or lipid-free apoA-I (*4*, *5*). While the role of ABCA1 in UC and phospholipid efflux has been studied extensively, the regulation of pre-β apoA-I formation is poorly understood.

Lipid-free or lipid-poor pre-β apoA-I dissociates from spherical HDL that are being remodeled by plasma factors such as phospholipid transfer protein and CETP (*6*, *7*). The present study establishes that pre-β apoA-I is generated during the CETP-mediated remodeling of rHDL and that the phospholipid composition of the particles plays a key role in these processes.

To carry out this study, it was important to use HDL that were comparable in size and lipid/protein ratio but varied systematically in phospholipid composition. This was achieved by developing a new approach for preparing spherical rHDL. These preparations proved to be excellent models for investigating pre-β apoA-I formation. They also gave a new insight into the CETP-mediated remodeling of HDL by showing that there is a high degree of cooperativity between the transfers that deplete the HDL of core lipids, the reduction in HDL size and the dissociation of apoA-I.

As the spherical rHDL CE acyl esters varied in length and unsaturation, it was important to establish that these differences did not affect either the remodeling of the

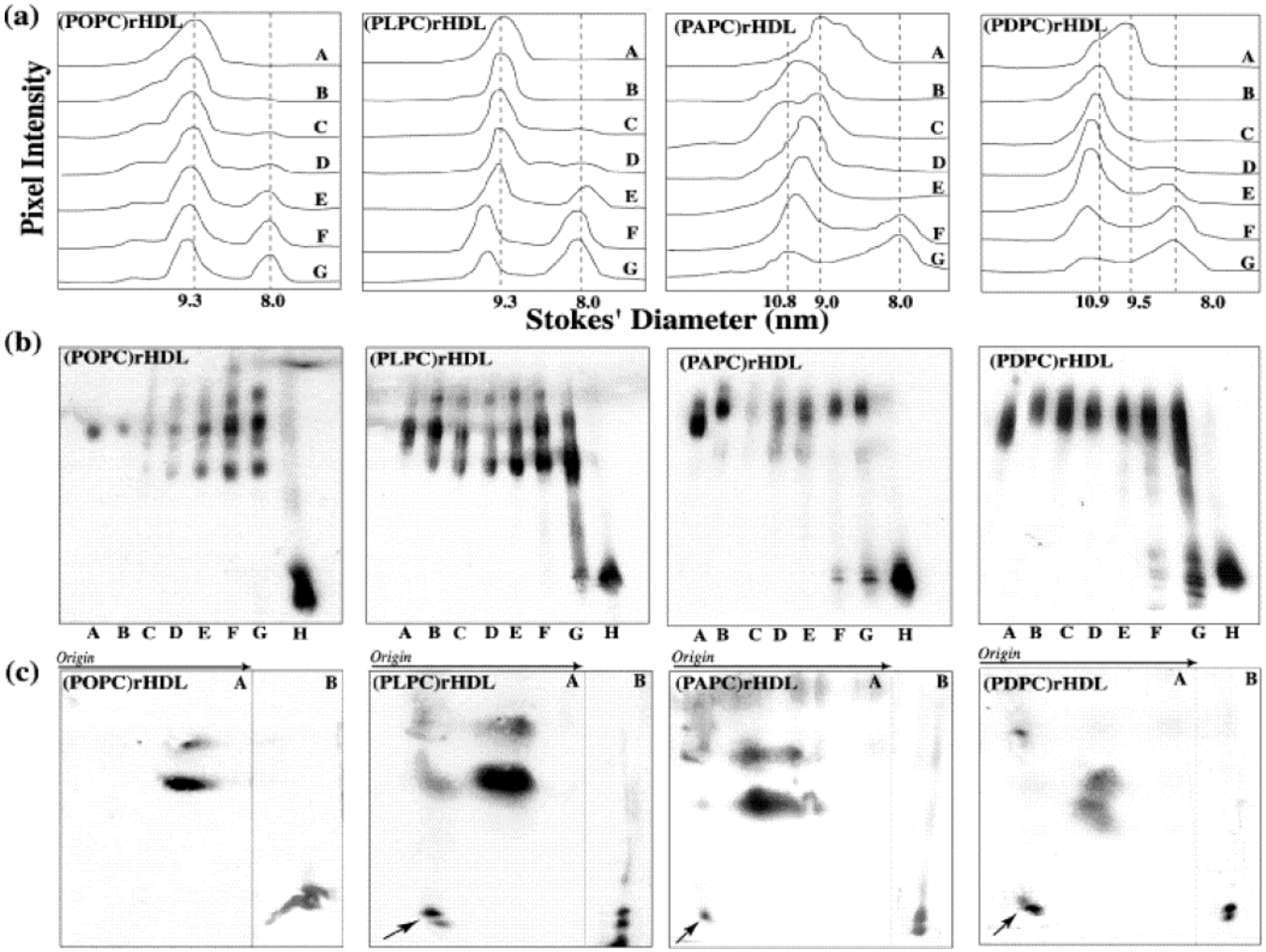

FIGURE 3: Remodeling of rHDL by CETP: Size changes and pre-β apoA-I formation. The rHDL and microemulsions were incubated with CETP as described for Figure 2. (a) Ultracentrifugally isolated rHDL were subjected to nondenaturing gradient gel electrophoresis. (b) Unprocessed incubation mixtures were electrophoresed on nondenaturing gradient gels, transferred to nitrocellulose membranes, and immunoblotted for apoA-I. Tracks A and B show rHDL's that were either maintained at 4 °C or incubated at 37 °C for 24 h with the microemulsions. Tracks C, D, E, F, and G respectively show rHDL incubated for 1, 3, 6, 12, and 24 h with microemulsions and CETP. Track H contains lipid-free apoA-I. (c) The rHDL and microemulsions were incubated for 24 h with CETP, subjected to 2-D gel electrophoresis and immunoblotted for apoA-I (panel A). Migration of the rHDL on the agarose gel is shown at the top of panel A. Panel B shows a sample of lipid-free apoA-I that was subjected to nondenaturing gradient gel electrophoresis only.

particles or pre-β apoA-I formation. This was achieved by enriching the (PLPC)rHDL, (PAPC)rHDL, and (PDPC)rHDL with CO. When the CO-enriched rHDL were incubated with CETP and the corresponding microemulsions, the remodeling of the rHDL and pre-β apoA-I formation were indistinguishable from what was found for the original, unmodified rHDL. It was therefore concluded that the length and unsaturation of cholesterol acyl esters does not impact on these processes. The observation that core lipid transfers between rHDL and microemulsions increased with increasing length and unsaturation of rHDL cholesterol acyl esters (Figure 2) is also consistent with this conclusion. If cholesterol acyl ester composition influenced the CETP-mediated remodeling of rHDL, core lipid transfers should decrease, not increase, with increasing acyl ester length and unsaturation.

The result showing that pre-β apoA-I was not formed during the CETP-mediated remodeling of (POPC)rHDL, despite the appearance of small particles in the incubation, was unexpected. This suggested that core lipid depletion must exceed a threshold level before dissociation of apoA-I occurs. It is also consistent with the stability of the apoA-I in (POPC)rHDL being enhanced relative to the apoA-I in the other rHDL preparations. The result in Figure 4, which shows that the unfolding of apoA-I in (POPC)rHDL is slow relative to the apoA-I in the other rHDL preparations, is consistent with this observation. This is probably due to the more ordered packing of the (POPC)rHDL phospholipid acyl chains enabling apoA-I to penetrate deeper into the rHDL surface.

One of the most interesting findings to emerge from this study is that pre-β apoA-I formation increases with increasing length and unsaturation of the rHDL PC *sn*-2 acyl chains. While this result can be explained entirely in terms of enhanced core lipid depletion of the particles, several lines of evidence suggest that it may also reflect the increasingly disordered rHDL PC acyl chains progressively destabilizing apoA-I by excluding it from the particle surface. This finding is of considerable physiological significance. The phospholipids in plasma HDL vary according to dietary fat intake (*23*) and following interactions with phospholipid transfer

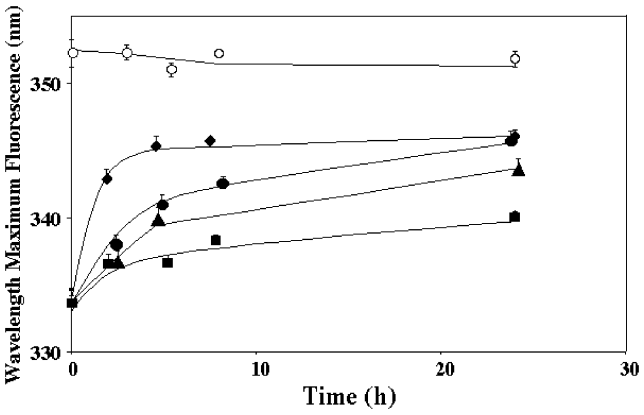

FIGURE 4: Unfolding of apoA-I. Spherical (POPC)rHDL (■), (PLPC)rHDL (▲), (PAPC)rHDL (●), (PDPC)rHDL (◆), and lipid-free apoA-I (○) were incubated for 0−24 h with 3.5 M GdnHCl. Wavelengths of maximum fluorescence were normalized to 333.7 nm at $T = 0$ h.

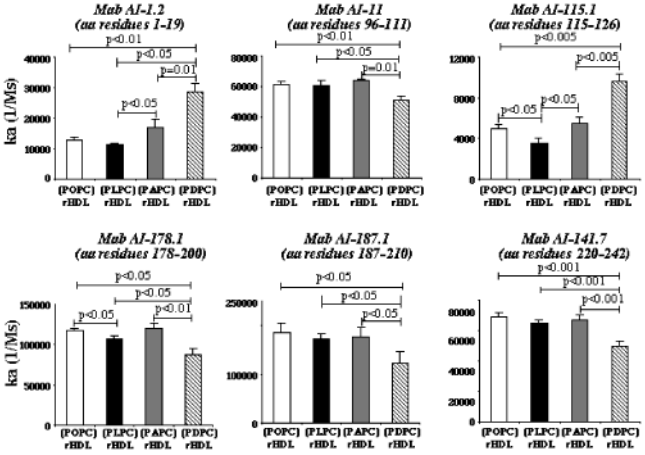

FIGURE 5: Binding of apoA-I-specific monoclonal antibodies to rHDL**.** Association rate constants (ka) (affinity) of six unique apoA-I-specific antibodies for (POPC)rHDL, (PLPC)rHDL, (PAPC)-rHDL, and (PDPC)rHDL were measured by surface plasmon resonance analysis. The apoA-I epitope defined by each antibody is identified by the amino acid residues of the mature protein.

protein and CETP (*7*, *24*). HDL also acquire phospholipids from chylomicrons that are undergoing lipolysis by lipoprotein lipase. The present results indicate that pre-β apoA-I formation may vary according to the acyl chain composition of the phospholipids that are incorporated into HDL by these processes.

This report also gives an insight into the capacity of CETP to generate pre-β apoA-I. The mass of pre-β apoA-I formed when the (PLPC)rHDL, (PAPC)rHDL and (PAPC)rHDL were incubated for 24 h with CETP and their respective microemulsions was estimated by scanning the immunoblots in Figure 3b and calculating the areas under the curves. Pre-β apoA-I accounted for 24%, 38%, and 35% of the total apoA-I in the (PLPC)rHDL, (PAPC)rHDL and (PAPC)rHDL incubations, respectively. The activity of CETP in plasma is about 40% of what was present in those incubations (see legend to Figure 2). Thus, to the extent that these in vitro findings reflect events that occur in vivo, the activity of CETP in normal human plasma has the potential to mediate the dissociation of 10−15% of the apoA-I from HDL each day. We have reported previously that the pre-β apoA-I that dissociates from HDL during incubation with CETP is essentially lipid-free (*6*). Given that lipid-free apoA-I is the preferred acceptor of the cholesterol that effluxes from peripheral cells via ABCA1 (*25*), it seems that the CETP-mediated generation of lipid-free apoA-I from HDL may make a substantial contribution to reverse cholesterol transport in vivo.

The pre-β apoA-I that dissociates from spherical HDL has several potential fates. It can accept cholesterol and phospholipids from cells and be converted into new spherical HDL by activity of LCAT. It may be incorporated directly into spherical HDL that are increasing in size following interaction with LCAT (*26*), or it may be removed from the circulation via the kidney (*27*). When these observations are considered in light of the present results, it follows that HDL phospholipids may be important for maintaining, and possibly increasing, HDL levels.

In conclusion, this study shows that phospholipids play a key role in pre-β apoA-I formation and the CETP-mediated remodeling of rHDL. They also regulate the accessibility and stability of apoA-I on the rHDL surface. The present results also raise, for the first time, the possibility that HDL phospholipids play a pivotal role in regulating plasma HDL levels and that they are important determinants of the initial step of reverse cholesterol transport.

ACKNOWLEDGMENT

K.A.R. is a Principal Research Fellow of the National Heart Foundation of Australia. The mass spectroscopic studies were carried out by Dr Chris Bagley (Hanson Institute, Adelaide, Australia).

REFERENCES

1. Mackness, M. I., Arrol, S., Abbott, C., and Durrington, P. N. (1993) *Atherosclerosis 104*, 129−135.
2. Cockerill, G. W., Rye, K.-A., Gamble, J. R., Vadas, M. A., and Barter, P. J. (1995) *Arterioscler. Thromb. Vasc. Biol. 15*, 1987−1994.
3. Barter, P. J., and Rye, K.-A. (1996) *Curr. Opin. Lipidol. 7*, 82−87.
4. Castro, G. R., and Fielding, C. J. (1988) *Biochemistry 27*, 25−29.
5. Rust, S., Rosier, M., Funke, H., Real, J., Amoura, Z., Piette, J.-C., Deleuze, J.-F., Brewer, H. B., Duverger, N., Denèfle, P., and Assmann, G. (1999) *Nat. Genet. 22*, 352−355.
6. Liang, H.-Q., Rye, K.-A., and Barter, P. J. (1994) *J. Lipid Res. 35*, 1187−1199.
7. Lusa, S., Jauhiainen, M., Metso, J., Somerharju, P., and Ehnholm, C. (1996) *Biochem. J. 313*, 275−282.
8. Davidson, W. S., Sparks, D. L., Lund-Katz, S., and Phillips, M. C. (1994) *J. Biol. Chem. 269*, 8959−8965.
9. Subbaiah, P. V., and Monshizadegan, H. (1988) *Biochim. Biophys. Acta 963*, 445−455.
10. Rye, K.-A., and Barter, P. J. (1994) *J. Biol. Chem. 269*, 10298−10303.
11. Osborne, J. C., Jr. (1986) *Methods Enzymol. 128*, 213−222.
12. Rye, K.-A., Hime, N. J., and Barter, P. J. (1996) *J. Biol. Chem. 271*, 4243−4250.
13. Rye, K.-A., Hime, N. J., and Barter, P. J. (1995) *J. Biol. Chem. 270*, 189−196.
14. Matz, C. E., and Jonas, A. (1982) *J. Biol. Chem. 257*, 4535−4540.
15. Parks, J. S., and Gebre, A. K. (1997) *J. Lipid Res. 38*, 266−275.
16. Martins, I. J., Lenzo, N. P., and Redgrave, T. G. (1989) *Biochim. Biophys. Acta. 1005*, 217−224.
17. Sattler W., Mohr D., and Stocker R. (1994) *Methods Enzymol. 233*, 469−489.
18. Curtiss, L. K., Bonnet, D. J., and Rye, K.-A. (2000) *Biochemistry 39*, 5712−5721.

19. Asztalos, B. F., Sloop, C. H., Wong, L., and Roheim, P. S. (1993) *Biochim. Biophys. Acta 1069*, 291−300.
20. Lowry, O. H., Rosebrough, N. J., Farr, A. L., and Randall, R. J. (1951) *J. Biol. Chem. 193*, 265−275.
21. Staros, J. V. (1982) *Biochemistry 21*, 3950−3955.
22. Huggins, K. W., Curtiss, L. K., Gebre, A. K., and Parks, J. S. (1998) *J. Lipid Res*. *39*, 2423−2431.
23. Sola, R., Motta, C., Maille, M., Bargallo, M. T., Boisnier, C., Richard, J. L., and Jacotot, B. (1993) *Arterioscler. Thromb. Vasc. Biol. 13*, 958−966.
24. Rye, K.-A., and Duong, M. N. (2000) *J. Lipid Res. 41*, 1640−1650.
25. Wang, N., Silver, D. L., Costet, P., and Tall,.R. (2000) *J. Biol. Chem. 275*, 33053−33058.
26. Liang, H.-Q., Rye, K.-A., and Barter, P. J. (1996) *J. Lipid Res. 37*, 1962−1970.
27. Horowitz, B. S., Goldberg, I. J., Merab J., Vannit, T., Ramakrishnan, R., and Ginsberg, H. N. (1992) in *High-Density Lipoproteins and Atherosclerosis III* (Miller, N. E., and Tall, A. R., Eds.), pp 215−222, Excerpta Medica, Amsterdam.

BI025998K